The Study of Complex Shapes of Fluid Membranes, the Helfrich Functional and New Applications

Zhong-Can Ou-Yang and Zhan-Chun Tu

Abstract The theoretical study of complex configurations of fluid membranes is reported on the basis of the Helfrich functional. Series of analytical results on the governing equations of closed lipid vesicles and open lipid vesicles with holes are surveyed. The concepts of stress tensor and moment tensor in fluid membranes are investigated from two different viewpoints: the balance of forces (moments) and the generalized variational principle of free energy. Several examples on new applications of the Helfrich functional in understanding the growth mechanism of some mesoscopic structures are illustrated.

Keywords Helfrich functional · Configuration · Membrane

Mathematics Subject Classification (2010). Primary 49Q10 · Secondary 53Z05

1 Introduction: From Soap Films to Red Blood Cells

There exist many structures whose one dimension is much smaller than the other two in our world. This kind of structures are usually called membranes, which may be thought of as 2-dimensional (2D) smooth surfaces in 3-dimensional (3D) Euclidean space. The identities formed by membranes display a variety of configurations. For example, soap bubbles at rest are always spherical; Human red blood cells are of biconcave discoid under the normal physiological condition.

The issue of equilibrium configurations of membranes has attracted much attention of mathematicians and physicists. As early as in 1803, Plateau investigated a soap film attaching to a metallic ring when the ring passed through soap water [1].

Z.-C. Ou-Yang
Institute of Theoretical Physics, Chinese Academy of Sciences, Beijing 100080, China
e-mail: oy@itp.ac.cn

Z.-C. Tu (✉)
Department of Physics, Beijing Normal University, Beijing 100875, China
e-mail: tuzc@bnu.edu.cn

T. Qian and L.G. Rodino (eds.), *Mathematical Analysis, Probability and Applications – Plenary Lectures*, Springer Proceedings in Mathematics & Statistics 177, DOI 10.1007/978-3-319-41945-9_4

He proposed that equilibrium configuration of the soap film corresponds to the minimum surface area of the film, which is mathematically equivalent to minimizing the functional

$$F = \int_M \mathrm{d}A, \tag{1.1}$$

where M and $\mathrm{d}A$ represent the membrane surface and the area element of the surface, respectively. The first-order variation of the Plateau functional (1.1) leads to a minimal surface with vanishing mean curvature $H = 0$. From 1805 to 1806, Young [2] and Laplace [3] studied soap bubbles. They proposed that the equilibrium configuration of a soap bubble corresponds to minimizing the surface area of the bubble for given volume enclosed in the bubble, which is mathematically equivalent to minimizing the functional

$$F = \lambda \int_M \mathrm{d}A + p \int \mathrm{d}V, \tag{1.2}$$

where λ and p represent the surface tension of the membrane and the osmotic pressure (pressure difference between the outer and the inner sides) of a soap bubble, respectively. $\mathrm{d}V$ represents the element of volume enclosed by the bubble. The first-order variation of the Young–Laplace functional (1.2) leads to a surface with constant mean curvature $H = p/2\lambda$. The reason that we can merely observe spherical bubbles is ascribed to the Alexandrov theorem—an embedded compact surface with constant mean curvature in 3D Euclidian space must be a spherical surface [4].

In 1812, Poisson [5] considered a solid shell and put forward an energy functional

$$F = \int_M H^2 \mathrm{d}A. \tag{1.3}$$

This functional was deeply investigated by Willmore [6, 7], thus, it is now called the Willmore functional in mathematics. Since the Willmore functional (1.3) is an invariant under conformal transformations, any configuration and its images under conformal transformations correspond to the same energy. The first-order variation of the Willmore functional (1.3) leads to

$$\nabla^2 H + 2H(H^2 - K) = 0, \tag{1.4}$$

a equation satisfied by the Willmore surfaces. The symbol K represents the Gauss curvature of the surface. The symbol ∇^2 represents the Laplace operator of the first kind defined on a 2D surface. Willmore showed that round spheres (as well as their images under conformal transformations) correspond to the least minimum of the Willmore functional (1.3) among all compact surfaces in 3D Euclidian space. In other words, all compact surfaces in 3D Euclidian space make the Willmore functional (1.3) to take values no less than 4π. Willmore further conjectured that all compact surfaces of genus one in 3D Euclidian space make the Willmore functional (1.3) to take values no less than $2\pi^2$, where the least minimum corresponds to the Willmore tori (as well

as their images under conformal transformations), which are special tori with the ratio of their two generation radii being $\sqrt{2}$ [8]. Recently, the Willmore conjecture has been proved by Marques and Neves via min-max theory [9].

Human red blood cells are unique since there are no internal cellular organelles inside the cells. They may be regarded as closed vesicles enclosed by cell membranes. In the energy scale of physiological condition, cell membranes are almost inextensible, and the volumes of red blood cells are hardly compressed. To explain the biconcave discoidal shape of red blood cells, Canham argued that the biconcave configuration might minimize the bending energy of membranes under the constraints of fixed area of membranes and fixed volume of the cells [10].

The cell membrane consists of lipid molecules and proteins, where lipid molecules form a bilayer while proteins are mosaicked in the bilayer [11]. In 1973, Helfrich recognized that the lipid bilayer is in the liquid crystal state at the physiological temperature. According to the elastic theory of liquid crystals, he proposed that the bending energy of the bilayer could be expressed as a functional

$$F_{\mathrm{H}} = \int_M [(k_c/2)(2H + c_0)^2 + \bar{k}K]\mathrm{d}A, \tag{1.5}$$

where $k_c > 0$ and $\bar{k}$ are two bending moduli of the bilayer [12]. The parameter c_0 represents the spontaneous curvature of the lipid bilayer, which reflects the asymmetric factors in the two leaflets of the bilayer. The numerical results implied that the biconcave configuration indeed minimizes the bending energy of the membrane under the constraints of fixed area of the membrane and fixed volume of the vesicle [13]. Henceforth, the elastic theory of lipid membranes based on the Helfrich functional (1.5) began to flourish [14–16]. In this review, we will survey several key theoretical results during the development of the elastic theory of lipid membranes according to our personal preferences. In Sect. 2, we will introduce a mathematical preliminary—calculus of variation in a deformable surface. In Sect. 3, we will present some theoretical results on configurations of closed lipid vesicles. In Sect. 4, we will present some theoretical results on configurations of open lipid vesicles with holes. In Sect. 5, we will discuss the concepts of stress tensor and moment tensor in fluid membranes. In Sect. 6, we will probe into new applications of the Helfrich functional and understand the growth mechanism of some mesoscopic structures. In the last section, we will give a brief summary and propose some perspectives.

2 Calculus of Variation in a Deformable Surface

In this section, we introduce the theory of surfaces and the variation problem in a deformable surface, which are based on the method of moving frames.

2.1 Theory of Surfaces Based on the Method of Moving Frames

Consider a 2D surface in 3D Euclidean space. Any point on the surface may be represented by a position vector $\mathbf{r}$. At point $\mathbf{r}$ we may construct a right-handed orthonormal frame $\{\mathbf{e}_1, \mathbf{e}_2, \mathbf{e}_3\}$ with $\mathbf{e}_3$ being the normal vector at that point. The set $\{\mathbf{r}; \mathbf{e}_1, \mathbf{e}_2, \mathbf{e}_3\}$ is called a moving frame.

The differentiation of the frame may be defined as [17]:

$$\mathrm{d}\mathbf{r} = \omega_1 \mathbf{e}_1 + \omega_2 \mathbf{e}_2, \tag{2.1}$$

and

$$\mathrm{d}\mathbf{e}_i = \omega_{ij} \mathbf{e}_j, \quad (i = 1, 2, 3) \tag{2.2}$$

where ω_1, ω_2, and $\omega_{ij} = \omega_{ji}$ $(i, j = 1, 2, 3)$ are 1-forms, and 'd' is the exterior differential operator. The repeated subscripts in this paper abide by the Einstein summation convention.

The area element can be expressed as [17]:

$$\mathrm{d}A \equiv \omega_1 \wedge \omega_2. \tag{2.3}$$

The structure equations of the surface can be expressed as [17]:

$$\begin{cases} \mathrm{d}\omega_1 = \omega_{12} \wedge \omega_2, \\ \mathrm{d}\omega_2 = \omega_{21} \wedge \omega_1, \\ \mathrm{d}\omega_{ij} = \omega_{ik} \wedge \omega_{kj} \quad (i, j = 1, 2, 3), \end{cases} \tag{2.4}$$

and

$$\begin{pmatrix} \omega_{13} \\ \omega_{23} \end{pmatrix} = \begin{pmatrix} a & b \\ b & c \end{pmatrix} \begin{pmatrix} \omega_1 \\ \omega_2 \end{pmatrix}. \tag{2.5}$$

Then we can define a curvature tensor as

$$\mathcal{C} = a\mathbf{e}_1\mathbf{e}_1 + b\mathbf{e}_1\mathbf{e}_2 + b\mathbf{e}_2\mathbf{e}_1 + c\mathbf{e}_2\mathbf{e}_2, \tag{2.6}$$

where $\mathbf{e}_i\mathbf{e}_j$ $(i, j = 1, 2)$ represents the dyad of $\mathbf{e}_i$ and $\mathbf{e}_j$. The mean curvature and the Gauss curvature are respectively defined as

$$H = \mathrm{tr}(\mathcal{C})/2 = (a + c)/2, \tag{2.7}$$

and

$$K = \det(\mathcal{C}) = ac - b^2. \tag{2.8}$$

For a curve on the surface, at each point in the curve we can construct the tangent vector $\mathbf{t}$. The normal curvature, the geodesic curvature, and the geodesic torsion of the curve may be expressed as

$$\kappa_n = a\cos^2\phi + 2b\cos\phi\sin\phi + c\sin^2\phi, \tag{2.9}$$

$$\tau_g = b\cos 2\phi + (c-a)\cos\phi\sin\phi \tag{2.10}$$

$$\kappa_g = (\mathrm{d}\phi + \omega_{12})/\mathrm{d}s \tag{2.11}$$

respectively, where ϕ represents the angle between $\mathbf{t}$ and $\mathbf{e}_1$.

2.2 *Calculus of Variations Based on the Method of Moving Frames*

Calculus of variation based on the method of moving frames was developed in the previous work by the present authors [18–20]. The main ideas are sketched as follows.

Any infinitesimal deformation of a surface can be achieved by a displacement vector

$$\delta\mathbf{r} \equiv \mathbf{\Omega} = \Omega_i\mathbf{e}_i \tag{2.12}$$

at each point on the surface, where δ can be understood as a variational operator. The frame is also changed due to the deformation of the surface. Its variation is denoted as

$$\delta\mathbf{e}_i = \Omega_{ij}\mathbf{e}_j \quad (i = 1, 2, 3), \tag{2.13}$$

where $\Omega_{ij} = -\Omega_{ji}$ $(i, j = 1, 2, 3)$. Ω_{23}, Ω_{31}, and Ω_{12} correspond to the infinitesimal rotation of the frame around direction $\mathbf{e}_1$, $\mathbf{e}_2$, and $\mathbf{e}_3$, respectively.

From $\delta\mathrm{d}\mathbf{r} = \mathrm{d}\delta\mathbf{r}$, $\delta\mathrm{d}\mathbf{e}_j = \mathrm{d}\delta\mathbf{e}_j$, we can derive:

$$\delta\omega_1 + \omega_2\Omega_{21} = \mathrm{d}\mathbf{\Omega}\cdot\mathbf{e}_1 = \mathrm{d}\Omega_1 + \Omega_2\omega_{21} + \Omega_3\omega_{31}, \tag{2.14}$$

$$\delta\omega_2 + \omega_1\Omega_{12} = \mathrm{d}\mathbf{\Omega}\cdot\mathbf{e}_2 = \mathrm{d}\Omega_2 + \Omega_1\omega_{12} + \Omega_3\omega_{32}, \tag{2.15}$$

$$\Omega_{13}\omega_1 + \Omega_{23}\omega_2 = \mathrm{d}\mathbf{\Omega}\cdot\mathbf{e}_3 = \mathrm{d}\Omega_3 + \Omega_1\omega_{13} + \Omega_2\omega_{23}, \tag{2.16}$$

$$\delta\omega_{ij} = \mathrm{d}\Omega_{ij} + \Omega_{il}\omega_{lj} - \omega_{il}\Omega_{lj}. \tag{2.17}$$

These equations are the essential equations of the variational method based on the moving frames.

With essential Eqs. (2.14)–(2.17), we may derive

$$\delta\mathrm{d}A = (\nabla\cdot\mathbf{\Omega} - 2H\Omega_3)\mathrm{d}A, \tag{2.18}$$

$$\delta(2H) = [\nabla^2 + (4H^2 - 2K)]\Omega_3 + \nabla(2H)\cdot\mathbf{\Omega}, \tag{2.19}$$

$$\delta K = \nabla \cdot \tilde{\nabla}\Omega_3 + 2KH\Omega_3 + \nabla K \cdot \mathbf{\Omega}. \tag{2.20}$$

In the above equations, the gradient operators and the Laplace operators are defined according to the differential operator, the Hodge star, and their generalizations as follows.

The 2D Hodge star operator $(*)$ satisfies $*\omega_1 = \omega_2$ and $*\omega_2 = -\omega_1$ [21]. The generalized Hodge star operator $(\tilde{*})$ satisfies $\tilde{*}\omega_{13} = \omega_{23}$ and $\tilde{*}\omega_{23} = -\omega_{13}$ [19]. The generalized differential operator $(\tilde{\mathrm{d}})$ satisfies $\tilde{\mathrm{d}}f = f_1\omega_{13} + f_2\omega_{23}$ if $\mathrm{d}f = f_1\omega_1 + f_2\omega_2$ [19]. Then, we may define the gradient operator (of the first kind) and the gradient operator of the second kind as [19]:

$$\nabla f \cdot \mathrm{d}\mathbf{r} = \mathrm{d}f, \tag{2.21}$$

and

$$\tilde{\nabla} f \cdot *\mathrm{d}\mathbf{r} = \tilde{*}\tilde{\mathrm{d}}f, \tag{2.22}$$

respectively. Simultaneously, we may define the Laplace operator (of the first kind) and the Laplace operator of the second kind as [19]:

$$(\nabla^2 f)\,\mathrm{d}A = \mathrm{d} * \mathrm{d}f, \tag{2.23}$$

and

$$(\nabla \cdot \tilde{\nabla} f)\,\mathrm{d}A = \mathrm{d}\tilde{*}\tilde{\mathrm{d}}f, \tag{2.24}$$

respectively.

Let us consider, a functional which depends on the mean curvature and the Gauss curvature of a surface. In general, the functional may be expressed as the following form:

$$F_G = \int_M G(2H, K)\mathrm{d}A, \tag{2.25}$$

where $G = G(2H, K)$ is a function of $2H$ and K. It is not hard to calculate the first-order variation of functional (2.25) by using Eqs. (2.18)–(2.20). From tedious calculations, we obtain

$$\begin{aligned}\delta F_G = &\int_M [\nabla^2 G_{2H} + \nabla \cdot \tilde{\nabla} G_K + (4H^2 - 2K)G_{2H} + 2HKG_K - 2HG]\Omega_3 \mathrm{d}A \\ &+ \oint_{\partial M} (G_{2H} * \mathrm{d}\Omega_3 - \Omega_3 * \mathrm{d}G_{2H} + G_K \tilde{*}\tilde{\mathrm{d}}\Omega_3 - \Omega_3 \tilde{*}\tilde{\mathrm{d}}G_K + G * \mathbf{\Omega} \cdot \mathrm{d}\mathbf{r}).\end{aligned} \tag{2.26}$$

where G_{2H} and G_K represent the partial derivatives of G with respect to $2H$ and K, respectively. $\oint_{\partial M}$ represents the integration along the boundary of surface M, which is vanishing for a closed surface.

3 Configurations of Closed Lipid Vesicles

As a model system, we will investigate configurations of a closed vesicle formed by a lipid bilayer. First, we will introduce the general shape equation for closed vesicles. Second, we will discuss the shape equation for axisymmetrical vesicles and its first integral. Finally, we will present several special solutions to the shape equation.

3.1 Energy Functional and the Corresponding Euler–Lagrange Equation

The bending energy of a closed vesicle may be described by the Helfrich functional (1.5). Since the area of lipid bilayer is almost inextensible and the volume of the closed vesicle is hardly compressed, we may introduce two Lagrange multipliers λ and p to replace these constraints. The extended energy functional of the closed vesicle may be expressed as

$$F = \int_M [(k_c/2)(2H + c_0)^2 + \bar{k}K + \lambda]\mathrm{d}A + pV, \tag{3.1}$$

where V represents the total volume enclosed in the vesicle. The Lagrange multiplier λ can be physically interpreted as the surface tension of the lipid bilayer. The Lagrange multiplier p can be regarded as the osmotic pressure of the vesicle, i.e., the pressure difference between the outer side and the inner side of the vesicle.

To derive the Euler–Lagrange equation corresponding to functional (3.1), we assume $G = (k_c/2)(2H + c_0)^2 + \bar{k}K + \lambda$. Substituting it into (2.26) and considering $\delta V = \int_M \Omega_3 \mathrm{d}A$, one can obtain

$$\delta F = \int_M [p - 2\lambda H + k_c(2H + c_0)(2H^2 - c_0 H - 2K) + 2k_c\nabla^2 H]\Omega_3. \tag{3.2}$$

The equilibrium configurations satisfy $\delta F = 0$, which leads to

$$p - 2\lambda H + k_c(2H + c_0)(2H^2 - c_0 H - 2K) + 2k_c\nabla^2 H = 0. \tag{3.3}$$

This equation was first derived by Ou-Yang and Helfrich [22, 23]. Now it is called the shape equation of lipid vesicles. Obviously, if $k_c = 0$, the above equation degenerates into the Young–Laplace equation $p - 2\lambda H = 0$. If $p = 0$ and $\lambda = 0$, the above equation degenerates into the Willmore Eq. (1.4).

3.2 Axisymmetrical Closed Vesicles

An axisymmetrical vesicle may be generated by its outline which is represented by $z = z(\rho)$ with ρ being the revolution radius. Take ϕ as the rotation angle and ψ as the tangent angle of the outline. The axisymmetrical vesicle may be parameterized as

$$x = \rho\cos\phi,\ \ y = \rho\sin\phi,\ \ z = \int \tan\psi(\rho)\mathrm{d}\rho. \tag{3.4}$$

According to Sect. 2, we can derive the mean curvature

$$H = -(\rho\sin\psi)'/2\rho, \tag{3.5}$$

the Gauss curvature

$$K = (\sin^2\psi)'/2\rho, \tag{3.6}$$

and the Laplace operator

$$\nabla^2 = \frac{1}{\rho^2}\frac{\partial^2}{\partial\phi^2} + \frac{\cos\psi}{\rho}\frac{\partial}{\partial\rho}\left(\rho\cos\psi\frac{\partial}{\partial\rho}\right). \tag{3.7}$$

Substituting the above three equations into the general shape Eq. (3.3), one can derive the shape equation for axisymmetrical vesicles:

$$\begin{aligned} &-\frac{\cos\psi}{\rho}\left\{\rho\cos\psi\left[\frac{(\rho\sin\psi)'}{\rho}\right]'\right\}' - \frac{1}{2}\left[\frac{(\rho\sin\psi)'}{\rho}\right]^3 \\ &+\frac{(\rho\sin\psi)'\left(\sin^2\psi\right)'}{\rho^2} - \frac{c_0\left(\sin^2\psi\right)'}{\rho} + \frac{\tilde{\lambda}\,(\rho\sin\psi)'}{\rho} + \tilde{p} = 0, \end{aligned} \tag{3.8}$$

where $\tilde{\lambda} \equiv \lambda/k_c + c_0^2/2$ and $\tilde{p} \equiv p/k_c$. In addition, the prime represents the derivative with respect to radius ρ. The above equation is a third-order ordinary differential equation, which was first derived by Hu and Ou-Yang [24]. It is found that the above equation is integrable [25]. This equation may be further transformed into a second-order ordinary differential equation:

$$\frac{\Psi^3 - \Psi(\rho\Psi')^2}{2\rho} - \rho(1-\Psi^2)\left[\frac{(\rho\Psi)'}{\rho}\right]' - c_0\Psi^2 + \tilde{\lambda}\rho\Psi + \frac{\tilde{p}\rho^2}{2} = \eta_0, \tag{3.9}$$

where $\Psi \equiv \sin\psi$ and η_0 being the first integral.

3.3 Analytical Special Solutions

The shape Eq. (3.3) and its axisymmetrical counterparts (3.8) and (3.9) are nonlinear differential equations, to which one cannot achieve general solutions. Till now, researchers have known some special solutions to these equations, such as minimal surfaces (including catenoid, helicoid, etc.), surfaces with constant mean curvature (including sphere, cylinder, unduloid [26, 27], etc.), Willmore surfaces (including Clifford torus [28], Dupin Cyclide [29], inverted catenoid [30], etc.), cylinder-like surfaces [31–33], and circular biconcave discoid [34, 35]. Among these solutions, only sphere, Clifford torus, Dupin cyclide, and circular biconcave discoid correspond to closed vesicles without self-intersections.

3.3.1 Sphere

The mean curvature and the Gauss curvature of a spherical surface with radius R are $H = -1/R$ and $K = 1/R^2$, respectively. Substituting them into the shape Eq. (3.3), one can derive

$$\tilde{p}R^2 + 2\tilde{\lambda}R - 2c_0 = 0. \tag{3.10}$$

This equation gives the relation between the radius R, the spontaneous curvature c_0, the reduced osmotic pressure $\tilde{p} \equiv p/k_c$, and the reduced surface tension $\tilde{\lambda} \equiv \lambda/k_c + c_0^2/2$. Obviously, if $\tilde{\lambda}^2 + 2c_0\tilde{p} < 0$, there is no spherical vesicle satisfying the shape equation. If $\tilde{\lambda}^2 + 2c_0\tilde{p} = 0$, there merely exists one spherical vesicle satisfying the shape equation. If $\tilde{\lambda}^2 + 2c_0\tilde{p} > 0$, there are two spherical vesicles satisfying the shape equation, which might correspond to the exocytosis or endocytosis of cells.

3.3.2 Clifford Torus

The Clifford torus is a revolution surface generated by a circle with radius r which rotates around an axis in the same plane of the circle. The revolution radius R should be larger than r. The torus may be parameterized as $\{(R + r\cos\varphi)\cos\phi, (R + r\cos\varphi)\sin\phi, r\sin\varphi\}$. The mean curvature and the Gauss curvature are $H = -(R + 2r\cos\varphi)/2r(R + r\cos\varphi)$ and $K = \cos\varphi/r(R + r\cos\varphi)$, respectively. Substituting them into the shape Eq. (3.3), one can derive $\tilde{\lambda} = 2c_0/r$, $\tilde{p} = -2c_0/r^2$, and

$$R/r = \sqrt{2}. \tag{3.11}$$

That is, there exists a lipid torus with the ratio of its two generation radii being $\sqrt{2}$ [28], which was confirmed in the experiment [36]. This kind of Clifford torus is called the Willmore torus [8] in mathematics. It is also found that nonaxisymmetric tori [37] constructed from conformal transformations of the Willmore torus also

satisfy the shape equation. In addition, it is not hard to check that $\eta_0 = -2c_0 - 1/r$ from equation (3.9) when $\tilde{\lambda} = 2c_0/r$, $\tilde{p} = -2c_0/r^2$, and $R/r = \sqrt{2}$.

3.3.3 Dupin Cyclide

The Dupin cyclide may be expressed as

$$(x^2 + y^2 + z^2 + a^2 - c^2 - \mu^2)^2 = 4(ax - c\mu)^2 + 4(a^2 - c^2)y^2, \tag{3.12}$$

where $a > \mu > c$ are three real parameters. Ou-Yang [29] found that the Dupin cyclide could satisfy the shape Eq. (3.3) when $p = 0$, $\lambda = 0$, $c_0 = 0$ and $\mu^2 = (a^2 + c^2)/2$. This kind of lipid vesicles were also observed in the experiment by Fourcade and his coworkers [38]. The Dupin cyclide and conformal transformations of the Willmore torus mentioned above are two classes of the few known asymmetric solutions to the shape Eq. (3.3) up to now.

3.3.4 Circular Biconcave Discoid

Naito et al. [34, 35] found that the parametric equation

$$\begin{cases} \Psi \equiv \sin\psi = -c_0\rho\ln(\rho/\rho_B) \\ z = z_0 + \int_0^\rho \tan\psi \mathrm{d}\rho \end{cases} \tag{3.13}$$

corresponds to the contour line of a circular biconcave discoid when $0 < |c_0\rho_B| <$ e. Substituting it into Eq. (3.9), one obtains $\tilde{p} = 0$, $\tilde{\lambda} = c_0^2/2$, and $\eta_0 = -2c_0 \neq 0$. Fitting the experimental results by Evans and Fung [39], Naito et al. obtained $c_0R_0 = -1.618$ where R_0 is the reduced radius of a red blood cell [35], i.e., $4\pi R_0^2$ corresponds to the surface area of the red blood cell. It is quite interesting that $c_0R_0 = -1.618 = -1/0.618$ happens to correspond the golden ratio.

4 Configurations of Open Lipid Vesicles with Holes

Open bilayer configurations can be stabilized by some proteins [40]. This experimental fact gave rise to investigating the configurations of lipid membranes with free exposed edges based on the Helfrich functional [18, 41–45].

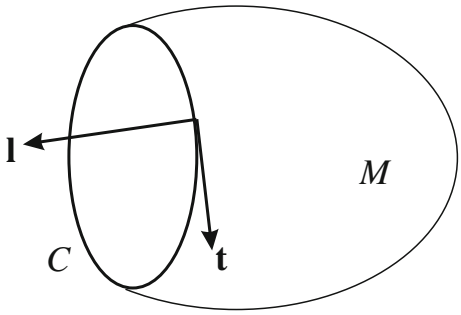

Fig. 1 An open smooth surface (M) with a boundary curve (C)

4.1 Energy Functional and the Corresponding Euler-Lagrange Equation

A lipid vesicle with a hole (i.e., a free edge) may be expressed as an open smooth surface M with a boundary curve $C = \partial M$ shown in Fig. 1. $\mathbf{t}$ represents the unit tangent vector of curve C. $\mathbf{l}$ is a unit vector which is perpendicular to $\mathbf{t}$ and the normal vector of the surface.

Based on the Helfrich functional, the energy functional for a lipid bilayer with a free edge may be expressed as

$$F = \int_M [(k_c/2)(2H + c_0)^2 + \bar{k}K + \lambda]\mathrm{d}A + \gamma \oint_C \mathrm{d}s, \tag{4.1}$$

where γ represents the line tension due to energy cost of the exposed edge. ds is the arc length element of curve C. According to the variational method in Sect. 2, from $\delta F = 0$ we can obtain the shape equation

$$2k_c\nabla^2 H + k_c(2H + c_0)(2H^2 - c_0 H - 2K) - 2\lambda H = 0, \tag{4.2}$$

and three boundary conditions [18, 41]

$$\left[k_c(2H + c_0) + \bar{k}\kappa_n\right]_C = 0, \tag{4.3}$$

$$\left[2k_c\partial H/\partial \mathbf{l} + \bar{k}\mathrm{d}\tau_g/\mathrm{d}s + \gamma\kappa_n\right]_C = 0, \tag{4.4}$$

$$\left[(k_c/2)(2H + c_0)^2 + \bar{k}K + \lambda + \gamma\kappa_g\right]_C = 0, \tag{4.5}$$

where κ_n, κ_g, and τ_g are the normal curvature, geodesic curvature, and geodesic torsion of the boundary curve, respectively. The above boundary conditions represent the force balance and the moment balance at each point in boundary curve C. They are also available for vesicles with more than one hole.

4.2 Axisymmetrical Situation

Consider an axisymmetric surface generated by a planar curve $z = z(\rho)$, which may be expressed as a vector form $\mathbf{r} = \{\rho\cos\phi, \rho\sin\phi, z(\rho)\}$ where ρ and ϕ are the rotation radius and azimuth angle, respectively. Under the axisymmetrical situation, the shape Eq. (4.2) is just the same as (3.8) with vanishing p. This equation is integrable and can be further transformed into

$$\frac{\Psi^3 - \Psi(\rho\Psi')^2}{2\rho} - \rho(1-\Psi^2)\left[\frac{(\rho\Psi)'}{\rho}\right]' - c_0\Psi^2 + \tilde{\lambda}\rho\Psi = \eta_0, \tag{4.6}$$

which is just the same as Eq. (3.9) with vanishing $\tilde{p}$.

For the boundary point C, we define a sign function $\sigma = \mathbf{t}\cdot\partial\mathbf{r}/\partial\phi$. The above boundary conditions (4.3)–(4.5) may be transformed into [18, 42]:

$$\Psi'|_C = c_0 - (1+\tilde{k})(\Psi/\rho)|_C, \tag{4.7}$$

$$\Psi''|_C = \left[\frac{\tilde{\gamma}\Psi}{\rho\sigma\cos\psi} + (2+\tilde{k})\frac{\Psi}{\rho^2} - \frac{c_0}{\rho}\right]_C, \tag{4.8}$$

$$\left[c_0\tilde{k}\left(\frac{\Psi}{\rho}\right) - \tilde{k}\left(1+\frac{\tilde{k}}{2}\right)\left(\frac{\Psi}{\rho}\right)^2 - \sigma\tilde{\gamma}\frac{\cos\psi}{\rho}\right]_C = \frac{c_0^2}{2} - \tilde{\lambda}, \tag{4.9}$$

where $\tilde{k} \equiv \bar{k}/k_c$, $\tilde{\gamma} \equiv \gamma/k_c$, $\Psi \equiv \sin\psi$, and $\tilde{\lambda} \equiv \lambda/k_c + c_0^2/2$. Since the boundary point is also in the surface, Eq. (4.6) should still hold for the boundary point C. From Eqs. (4.8) and (4.9) we can eliminate $\tilde{\gamma}$ and obtain the expression of $\Psi''|_C$. Substituting it and Eq. (4.7) into (4.6), we obtain a compatibility condition between the shape equation and boundary conditions for axisymmetrical open lipid vesicles:

$$\eta_0 = 0. \tag{4.10}$$

Under this condition, the above boundary conditions are not independent of each other. We may keep Eqs. (4.7) and (4.9) as boundary conditions. The shape equation may be expressed as (4.6) with vanishing η_0.

4.3 Analytical Special Solutions

Since the shape equation and boundary conditions are nonlinear, one may take the following procedure to find analytical special solutions: (i) finding a surface satisfying the shape equation; (ii) finding a curve C on that surface such that the boundary conditions are satisfied; (iii) the domain enclosed by boundary curve C on that surface being the solution. However, for a given surface satisfying the shape equation, we may not always find a curve C on that surface such that the boundary conditions

are satisfied. On what kind of surface satisfying the shape equation can we find a curve C such that the boundary conditions are satisfied? This issue was named as compatibility between the shape equation and boundary conditions [42]. For example, the compatibility condition for axisymmetrical solutions is just Eq. (4.10), i.e., the vanishing first integral.

In general case without axisymmetry, we may obtain the compatibility condition [42]

$$2\int_M (c_0 H + \tilde{\lambda})\mathrm{d}A + \tilde{\gamma}\oint_C \mathrm{d}s = 0. \tag{4.11}$$

through scaling analysis. Here, we do not exclude the possibility to achieve the other compatibility conditions through specific method. Using the compatibility conditions (4.10) and (4.11), we can verify a theorem of nonexistence [42, 45]: For finite line tension, there does NOT exist an open membrane being a part of surfaces with nonvanishing constant mean curvature (including sphere, cylinder, and unduloid etc.), Willmore surfaces (including Willmore torus, Dupin cyclide, and inverted catenoid etc.), and circular biconcave discoid.

The above theorem of nonexistence merely leaves a small window for the surfaces simultaneously satisfying the shape equation and the boundary conditions that we have known till now. When c_0 is vanishing, the shape equation holds for minimal surfaces. Three boundary conditions (4.3)–(4.5) are degenerated to

$$\kappa_n = 0,\ \kappa_g = -\lambda/\gamma = \text{constant}, \tag{4.12}$$

which implies that the boundary should be an asymptotic curve with constant geodesic curvature. A domain in a minimal surface with a smooth boundary being an asymptotic curve with constant geodesic curvature is called a minimal geodesic disk. Obviously, a planar circular disk is a trivially minimal geodesic disk since a plane is a special minimal surface with vanishing Gauss curvature. We have conjecture that a planar disk is the unique minimal geodesic disk [46, 47]. This conjecture is probably true. Recently, we have noted that, following the work on flat points of minimal surfaces by Koch and Fischer [48], Giomi and Mahadevan argued that there does not exist a simple domain bounded by a smooth asymptotic curve in a minimal surface with nonvanishing Gauss curvature [49]. If their argument is true, then our conjecture is straightforward since a circle in a plane is the unique planar curve with constant geodesic curvature.

5 Stress Tensor and Moment Tensor in Fluid Membranes

The concepts of stress tensor and moment tensor in fluid membranes were mainly developed by Guven and his coworkers [50–53]. These concepts may be used to derive the boundary conditions of an open lipid vesicle with a hole [41] and the linking conditions of a lipid vesicle with two-phase domains [54].

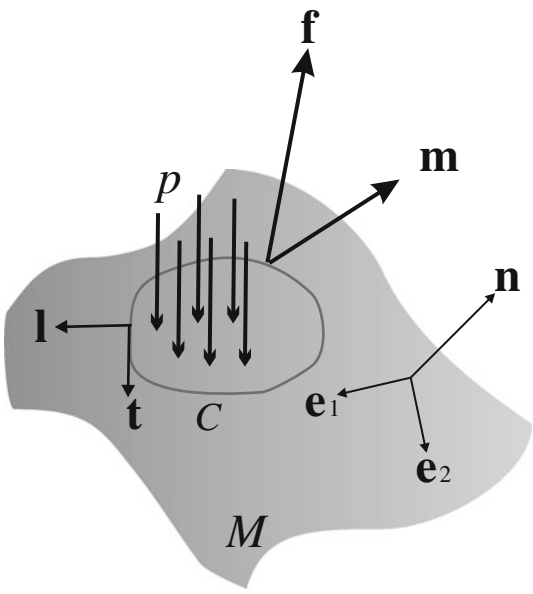

Fig. 2 Force and moment loaded on a domain cut from a fluid membrane

5.1 Balances of Local Forces and Moments

The concepts of stress tensor and moment tensor come from the force balance and the moment balance for any domain in a lipid membrane. As shown in Fig. 2, we cut a domain D bounded by a curve C from the lipid membrane. $\{\mathbf{e}_1, \mathbf{e}_2, \mathbf{n}\}$ is a right-handed orthogonal frame with $\mathbf{n} \equiv \mathbf{e}_3$ being the unit normal vector of the surface. A pressure p is loaded on the surface against the normal direction. The notations of $\mathbf{t}$ and $\mathbf{l}$ are the same as those in the above section. Vectors $\mathbf{f}$ and $\mathbf{m}$, respectively represent the density of force and the density of moment loaded on curve C by the lipids outside the domain.

According to Newtonian mechanics, the force balance and the moment balance may be expressed as

$$\oint_C \mathbf{f} \mathrm{d}s - \int p\mathbf{n} \mathrm{d}A = 0, \tag{5.1}$$

$$\oint_C \mathbf{m} \mathrm{d}s + \oint_C \mathbf{r} \times \mathbf{f} \mathrm{d}s - \int \mathbf{r} \times p\mathbf{n} \mathrm{d}A = 0. \tag{5.2}$$

If defining two second-order tensors $\mathcal{S}$ and $\mathcal{M}$ such that

$$\mathcal{S} \cdot \mathbf{l} = \mathbf{f}, \text{ and } \mathcal{M} \cdot \mathbf{l} = \mathbf{m}, \tag{5.3}$$

one can derive the equilibrium equations [20]:

$$\operatorname{div} \mathcal{S} = p\mathbf{n}, \tag{5.4}$$

$$\operatorname{div} \mathcal{M} = \mathcal{S}_1 \times \mathbf{e}_1 + \mathcal{S}_2 \times \mathbf{e}_2, \tag{5.5}$$

with $\mathcal{S}_1 \equiv \mathcal{S} \cdot \mathbf{e}_1$ and $\mathcal{S}_2 \equiv \mathcal{S} \cdot \mathbf{e}_2$ from the Stokes theorem. The tensors $\mathcal{S}$ and $\mathcal{M}$ are called the stress tensor and the moment tensor, respectively.

5.2 Explicit Expressions of Stress Tensor and Moment Tensor

One may understand the equilibrium configuration of the cut lipid domain D in Fig. 2 from the point of energy view. That is, the equilibrium configuration abides by the following generalized variational principle [54]:

$$\begin{aligned} &\delta \int_D [(k_c/2)(2H + c_0)^2 + \bar{k}K + \lambda] \mathrm{d}A \\ &+ \int_D p\mathbf{n} \cdot \mathbf{\Omega} \mathrm{d}A - \oint_C \mathbf{f} \cdot \mathbf{\Omega} \mathrm{d}s - \oint_C \mathbf{m} \cdot \mathbf{\Theta} \mathrm{d}s \\ &+ \oint \mu[\Theta_1\omega_2 - \Theta_2\omega_1 - \Omega_1\omega_{13} - \Omega_2\omega_{23} - \mathrm{d}\Omega_3] = 0 \end{aligned} \tag{5.6}$$

The first line of the above equation represents the variation of bending energy of the lipid bilayer. The second line of the above equation reflects the potential energy increment due to the external loads. In the third line of the above equation, μ is a Lagrange multiplier due to the geometric constraint (2.16). The angular vector is defined as $\mathbf{\Theta} \equiv \Theta_i \mathbf{e}_i \equiv \Omega_{23}\mathbf{e}_1 + \Omega_{31}\mathbf{e}_2 + \Omega_{12}\mathbf{e}_3$.

Using the variational method mentioned in Sect. 2 and considering the definition (5.3), one can derive the explicit expressions of stress tensor and moment tensor as follows [54]:

$$\mathcal{S} = [(k_c/2)(2H + c_0)^2 + \lambda]\mathcal{I} - k_c(2H + c_0)\mathcal{C} - 2k_c\mathbf{n}\nabla H - (\mu\mathcal{C} - \mathbf{n}\nabla\mu) \times \mathbf{n}, \tag{5.7}$$

and

$$\mathcal{M} = \mu\mathcal{I} - [k_c(2H + c_0)\mathcal{I} + \bar{k}\mathcal{C}] \times \mathbf{n}, \tag{5.8}$$

where $\mathcal{I} \equiv \mathbf{e}_1\mathbf{e}_1 + \mathbf{e}_2\mathbf{e}_2$ represents the unit tensor, and $\mathcal{C}$ is the curvature tensor (2.6). It is not hard to verify that (5.5) automatically holds from the above two equations while Eq. (5.4) is equivalent to the shape Eq. (3.3). Substituting Eqs. (5.7) and (5.8) into (5.3), one may obtain the force and moment on the boundary C [54]:

$$\begin{aligned} \mathbf{f} = &[k_c(2H + c_0)\tau_g - \mu\kappa_n]\mathbf{t} + [\nabla\mu \cdot \mathbf{t} - 2k_c\nabla H \cdot \mathbf{l}]\mathbf{n} \\ &+ [k_c(2H + c_0)(c_0/2 - H + \kappa_n) + \lambda + \mu\tau_g]\mathbf{l}, \end{aligned} \tag{5.9}$$

and

$$\mathbf{m} = -[k_c(2H + c_0) + \bar{k}\kappa_n]\mathbf{t} + (\mu + \bar{k}\tau_g)\mathbf{l}, \tag{5.10}$$

where κ_n and τ_g represents the normal curvature and the geodesic torsion of the boundary, respectively.

Here two remarks should be mentioned. First, we only present the expressions of $\mathcal{S}$, $\mathcal{M}$, $\mathbf{f}$, and $\mathbf{m}$ based on the Helfrich functional. Their general forms can be found in Ref. [54]. Second, there is a Lagrange multiplier μ in the above expressions, which comes from the geometric constraint (2.16). Its physical meaning is still unknown. The terms related to μ in the expressions of $\mathcal{S}$, $\mathcal{M}$, $\mathbf{f}$, and $\mathbf{m}$ have not been included in the previous researches [20, 47, 50–53].

5.3 *Simple Applications of Stress Tensor and Moment Tensor*

Here, we will survey two applications of the concepts of stress tensor and moment tensor. One is the derivation of the boundary conditions of an open lipid vesicle with a hole [41]; another is the derivation of the linking conditions of a lipid vesicle with two-phase domains [54]. The basic ideas are as follows.

Consider a string loaded by a force density $\mathbf{f}$ and a moment density $\mathbf{m}$. The line tension γ induces a stretching force along the tangent vector of the string. From the force balance and the moment balance, one can easily derive two equilibrium equations [54]:

$$\gamma\kappa(s)\mathbf{N} + \mathbf{f}(s) = 0, \tag{5.11}$$

$$\mathbf{m}(s) = 0, \tag{5.12}$$

where s is the arc length parameter of the string. $\kappa(s)$ is the curvature of the string at s.

Now cut a very thin ribbon along the edge from the membrane as shown in Fig. 3. $\mathbf{t}$ and $\mathbf{t}_i$ represent the tangent vector of the boundary curve and that of the cutting line, respectively. $\mathbf{l}$ is perpendicular to the normal vector of membrane surface and the tangent vector of the boundary curve. $\mathbf{l}_i$ is perpendicular to the normal vector of membrane surface and the tangent vector of the cutting line. $\mathbf{f}$ and $\mathbf{m}$ represent the force density and the moment density induced by the membrane, respectively. Since $\mathbf{t}_i = -\mathbf{t}$ and $\mathbf{l}_i = -\mathbf{l}$, according Eqs. (5.9) and (5.10), we have

$$\begin{aligned}\mathbf{f} = &-[k_c(2H + c_0)\tau_g - \mu\kappa_n]\mathbf{t} - [\nabla\mu \cdot \mathbf{t} - 2k_c\nabla H \cdot \mathbf{l}]\mathbf{n} \\ &- [k_c(2H + c_0)(c_0/2 - H + \kappa_n) + \lambda + \mu\tau_g]\mathbf{l},\end{aligned} \tag{5.13}$$

and

$$\mathbf{m} = [k_c(2H + c_0) + \bar{k}\kappa_n]\mathbf{t} - (\mu + \bar{k}\tau_g)\mathbf{l}. \tag{5.14}$$

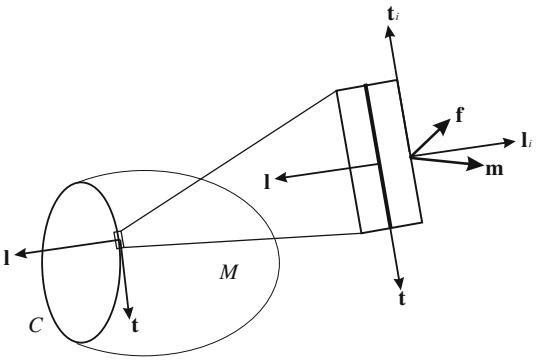

Fig. 3 Thin ribbon cut from the membrane along the edge

Substituting Eq. (5.14) into (5.12), we can obtain

$$\mu = -\bar{k}\tau_g, \tag{5.15}$$

and the boundary condition (4.3). If we substituting Eqs. (4.3) and (5.15) into (5.13), the force density is transformed into

$$\mathbf{f} = -[(k_c/2)(2H + c_0)^2 + \bar{k}K + \lambda]\mathbf{l} + [\bar{k}\mathrm{d}\tau_g/\mathrm{d}s + 2k_c\partial H/\partial \mathbf{l}]\mathbf{n}. \tag{5.16}$$

In the above derivation, we have used $\mathrm{d}\tau_g/\mathrm{d}s = \nabla\tau_g \cdot \mathbf{t}$, $\partial H/\partial \mathbf{l} = \nabla H \cdot \mathbf{l}$, and $(2H - \kappa_n)\kappa_n - \tau_g^2 = K$. Substituting Eq. (5.16) into (5.11) and considering $\kappa_n = \kappa\mathbf{n} \cdot \mathbf{N}$ and $\kappa_g = -\kappa\mathbf{l} \cdot \mathbf{N}$, we can obtain the boundary conditions (4.4) and (4.5).

Similar procedure is also available to derive the linking conditions of a lipid vesicle with two-phase domains as shown in Fig. 4. The separation line between domain I (D^{I}) and domain II (D^{II}) is denoted as curve C. $\mathbf{t}$ is the tangent vector of curve C. $\mathbf{l}^{\mathrm{I}}$ is perpendicular to $\mathbf{t}$ and the normal vector of surface. Different from Fig. 1, $\mathbf{l}^{\mathrm{I}}$ points to the side of domain I. The definition of $\mathbf{l}^{\mathrm{II}}$ is similar. The subtle difference is that $\mathbf{l}^{\mathrm{II}}$ points to the side of domain II. Assume that the membrane surface is so smooth that $\mathbf{l}^{\mathrm{II}} = -\mathbf{l}^{\mathrm{I}}$.

An axisymmetrical vesicle with two-phase domains was investigated by Jülicher and Lipowsky [55] many years ago. The general cases without the axisymmetrical

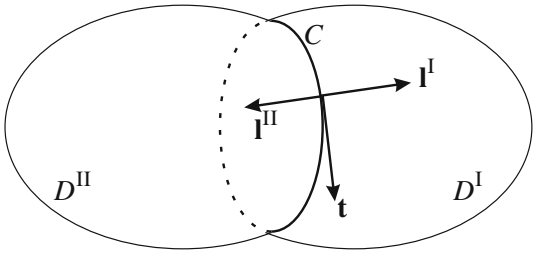

Fig. 4 A lipid vesicle with two-phase domains

precondition have also been discussed by several researchers in recent years [19, 54, 56]. Following the Helfrich functional, the free energy of a lipid vesicle with two-phase domains may be expressed as [55]

$$F = \sum_{i=\mathrm{I}}^{\mathrm{II}} \int_{D^i} [(k_c^i/2)(2H^i + c_0^i)^2 + \bar{k}^i K^i + \lambda^i] \mathrm{d}A^i + pV + \gamma \oint_C \mathrm{d}s, \quad (5.17)$$

where superscript i labels the quantities of domain i ($i = \mathrm{I}, \mathrm{II}$). The linking conditions of separation curve C may also be derived from the concepts of stress tensor and moment tensor, which are listed as follows [54]:

$$k_c^{\mathrm{I}}(2H^{\mathrm{I}} + c_0^{\mathrm{I}}) + \bar{k}^{\mathrm{I}}\kappa_n = k_c^{\mathrm{II}}(2H^{\mathrm{II}} + c_0^{\mathrm{II}}) + \bar{k}^{\mathrm{II}}\kappa_n, \quad (5.18)$$

$$\frac{\partial \left[k_c^{\mathrm{I}}(2H^{\mathrm{I}} + c_0^{\mathrm{I}})\right]}{\partial \mathbf{l}^{\mathrm{I}}} + \frac{\partial \left[k_c^{\mathrm{II}}(2H^{\mathrm{II}} + c_0^{\mathrm{II}})\right]}{\partial \mathbf{l}^{\mathrm{II}}} = (\bar{k}^{\mathrm{I}} - \bar{k}^{\mathrm{II}})\frac{\mathrm{d}\tau_g}{\mathrm{d}s} + \gamma\kappa_n, \quad (5.19)$$

and

$$\frac{k_c^{\mathrm{I}}}{2}(4H^{\mathrm{I}2} - c_0^{\mathrm{I}2}) - \frac{k_c^{\mathrm{II}}}{2}(4H^{\mathrm{II}2} - c_0^{\mathrm{II}2}) + (\bar{k}^{\mathrm{I}} - \bar{k}^{\mathrm{II}})\left(\kappa_n^2 + \tau_g^2\right) = \lambda^{\mathrm{I}} - \lambda^{\mathrm{II}} + \gamma\kappa_g. \quad (5.20)$$

It should be noted that the mean curvature could be discontinuous across the separation curve. Using the above linking conditions, the Jülicher-Lipowsky conjecture on the general neck condition for the limit shape of budding vesicles was verified [54].

6 Understanding the Growth Mechanism of Some Mesoscopic Structures Based on the Helfrich Functional

The growth of mesoscopic structures is different from that of macroscopic structures. Macroscopic structures usually correspond to the least minimal free energy. But in the mesoscopic scale, there is no enough time for the structures to release energy as heat. Thus most mesoscopic structures exist in a metastable state where the different kinds of energies are balanced each other. With the consideration of the Helfrich functional, this idea has been used to explain the formation of focal conic domain in smectic-A liquid crystals [57, 58], the pitch angle of helices of multi-walled carbon nanotubes [59], and the reversible transition between peptide nanotubes and spherical vesicles [60].

6.1 Focal Conic Domain in Smectic-A Liquid Crystals

In Smectic-A (SmA) liquid crystals [61], the molecules are stacked layer-by-layer. In each layer, the orientations of all molecules are aligned to the normal of the layer. Generally, the flat configuration is energetically favorable. However, Dupin cyclides are usually formed when liquid crystals cool from the isotropic (Iso) phase to the SmA phase. Series of Dupin cyclides constitute a focal conic domain. Bragg argued that "There must be a reason why the cyclides are preferred, and it must be based on energy considerations" [62]. Natio et al. proposed that the relieved energy of the difference in the Gibbs free energy of Iso-SmA transition must be balanced by the curvature elastic energy of the smectic layers [58].

The formation energy of a focal conic domain includes three kinds of contributions. First is the volume free energy change due to the Iso-SmA transition [57]:

$$F_V = -g_0 \oint (D - D^2 H + D^3 K/3) \mathrm{d}A, \tag{6.1}$$

where $g_0 > 0$ is the difference in the Gibbs free energy density between SmA and Iso phases. H and K represent the mean and Gauss curvatures of the inner surface, respectively. Second is the surface energy of inner and outer SmA-Iso interfaces [58]:

$$F_A = \lambda \oint (1 + |1 - 2DH + D^2 K|) \mathrm{d}A, \tag{6.2}$$

where λ is the surface energy per area. Third is the curvature elastic energy, which is the sum of the energy (in the Helfrich form) of each layers. In the continuum limit, the curvature elastic energy may be expressed as [58]:

$$F_c = k_c \oint \sqrt{H^2 - K} \ln\left(\frac{1 - DH + D\sqrt{H^2 - K}}{1 - DH - D\sqrt{H^2 - K}}\right) \mathrm{d}A + \bar{k} D \oint K \mathrm{d}A. \tag{6.3}$$

Then the total formation energy may be expressed as $F = F_V + F_A + F_c \oint \Phi(H, K, D) \mathrm{d}A$ with

$$\begin{aligned} \Phi(H, K, D) \equiv k_c \sqrt{H^2 - K} \ln\left(\frac{1 - DH + D\sqrt{H^2 - K}}{1 - DH - D\sqrt{H^2 - K}}\right) + \bar{k} D K \\ + \lambda(1 + |1 - 2DH + D^2 K|) - g_0(D - D^2 H + D^3 K/3). \end{aligned} \tag{6.4}$$

From $\delta F = 0$, Natio et al. obtained

$$(\nabla^2/2)\Phi_H + \nabla \cdot \tilde{\nabla} \Phi_K + (2H^2 - K)\Phi_H + 2HK\Phi_K - 2H\Phi = 0 \tag{6.5}$$

and

$$\oint \Phi_D \mathrm{d}A = 0, \tag{6.6}$$

where $\Phi_H \equiv \partial\Phi/\partial H$, $\Phi_K \equiv \partial\Phi/\partial K$, and $\Phi_D \equiv \partial\Phi/\partial D$. ∇^2 and $\nabla \cdot \tilde{\nabla}$ are the Laplace operators mentioned in Sect. 2. Natio et al. showed that the growth of the focal conic domain in SmA liquid crystals could be well explained by using the above two equations [58].

6.2 Helices of Multi-walled Carbon Nanotubes

The formation mechanism of a multi-walled carbon nanotube is similar to that of focal conic domain in SmA liquid crystals mentioned above. The formation energy of the multi-walled carbon nanotube also consists of three terms: (i) the volume term which may be expressed in the same form of (6.1); (ii) the surface term which may be expressed as the same form of (6.2); (iii) the curvature energy which may be expressed as the same form of (6.3) since the bending energy of a single layer of graphene was proven to have the Helfrich form [59]. If considering that the radius of the carbon nanotube is much smaller than the curvature radius of the central axis of the carbon nanotube, the total formation energy may be transformed into

$$F = m \int \mathrm{d}s + \alpha \int \kappa^2 \mathrm{d}s, \tag{6.7}$$

where m and α are two elastic constants. κ and s represent the curvature and the arc length of the central axis of the carbon nanotube, respectively. The first-order variation $\delta F = 0$ yields the equilibrium-shape equations of a string [63]:

$$2\mathrm{d}^2\kappa/\mathrm{d}s^2 + \kappa^3 - 2\kappa\tau^2 - (m/\alpha)\kappa = 0, \tag{6.8}$$

$$\kappa^2\tau = \text{constant}. \tag{6.9}$$

One solution to the above shape equations is a straight multi-walled carbon nanotube with vanishing κ and τ. The other solution to the above shape equations is a helix with pitch angle θ. From Eqs. (6.8) and (6.7), one may calculate the total formation energy for the helix

$$F = ml[1 + 1/(1 - 2\tan^2\theta)], \tag{6.10}$$

where l represents the total length of the central axis of the helix. The threshold condition for formation of helix is $F = 0$, which requires $\theta = \pi/4$. This value is in a good agreement with the pitch angle observed in the experiment [64].

6.3 Reversible Transition Between Peptide Nanotubes and Spherical Vesicles

In recent work, Yan et al. have observed the reversible transition between peptide nanotubes and vesicle-like structures [60]. It was found that the dilution of a peptide-nanotube dispersion solution results in the formation of vesicle-like structures, which can be reassembled into the nanotubes by concentrating the solution [60]. The mechanism underlying these phenomena is the same as the formation of the focal conic domain in SmA liquid crystals mentioned above.

As shown in reference [57], the outward growth of a layer with small thickness h on the top of the outermost equilibrium dipeptide aggregate (the nanotube or vesicle-like structure) leads to three kinds of free energy accumulations. First is the increment of the volume free energy:

$$F_V = -g_0 \oint (h - h^2 H + h^3 K/3) \mathrm{d}A, \tag{6.11}$$

where H and K are the mean curvature and the Gauss curvature of the outer surface of the dipeptide aggregate, respectively. g_0 is the difference in the Gibbs free energy density between the solution phase and the aggregate phase. Its value could be estimated with the ideal gas model, which reads

$$g_0 = C_A k_B T \ln(C_A/C_S), \tag{6.12}$$

where C_A and C_S are the concentrations of dipeptide in the aggregate phase and the solution phase, respectively [60]. k_B and T are the Boltzman constant and the temperature of the solution. Second is the extra interfacial free energy:

$$F_A = \lambda \oint (-2hH + h^2 K) \mathrm{d}A, \tag{6.13}$$

where λ is the surface energy per area of the solution/aggregate interface. Third is the extra curvature elastic energy, which can be expressed as the Helfrich form [57]:

$$F_c = \frac{k_1 h}{2} \oint (2H)^2 \mathrm{d}A + k_5 h \oint K \mathrm{d}A, \tag{6.14}$$

where k_1 and k_5 are related to the elastic constants of liquid crystals.

The equilibrium shape of the aggregate should satisfy $\partial F/\partial h = 0$, which leads to the Weingarten equation

$$2k_1 H^2 + k_5 K - g_0 - 2\lambda H = 0. \tag{6.15}$$

It is easy to verify that a sphere of radius r_0 and a cylinder of radius ρ_0 are two solutions to Eq. (6.15) provided that

$$r_0 = \frac{2k_1 + k_5}{\sqrt{\lambda^2 + g_0(2k_1 + k_5)} - \lambda} \approx \frac{2\lambda}{g_0}, \tag{6.16}$$

and

$$\rho_0 = \frac{k_1}{\sqrt{\lambda^2 + 2g_0k_1} - \lambda} \approx \frac{\lambda}{g_0}. \tag{6.17}$$

The approximations in the above two equations have been done according to the experiment conditions [60]. From these equations, one can calculate the formation energy of sphere and tube, respectively. The results are $F_{\text{shpere}} = -(g_0^3h^3/12\lambda^2 + g_0^2h^2/4\lambda)$ and $F_{\text{tube}} = -g_0^2h^2/2\lambda$. Thus, the condition for transition from a tube-to-a spherical structure is $F_{\text{tube}} > F_{\text{shpere}}$, that is, $g_0h > 3\lambda$. Substituting $g_0h = 3\lambda$ into Eq. (6.12) one can obtain the critical concentration for tube-to-vesicle-transition [60]

$$C_* = C_A \exp(-3\lambda/C_Ahk_BT). \tag{6.18}$$

When $C_S < C_*$, peptide nanotubes will transform into spherical vesicle-like structures.

7 Conclusion

In the above discussions, we have presented several theoretical investigations based on the Helfrich functional (1.5). The configurations of closed lipid vesicles and open lipid vesicles with holes, and the concepts of stress tensor and moment tensor in fluid membranes were surveyed in detail. It was shown that the Helfrich functional could be extended to understand the growth mechanism of some mesoscopic structures.

The study of the Willmore functional (1.3) enters the epilog stage as the Willmore conjecture has been proved [9]. We believe that the times of studying the Helfrich functional is coming soon. Although the aforementioned theoretical achievements based on the Helfrich functional have been made in recent years, the substantial researches on the Helfrich functional are still in their infancy. If $c_0 > 0$, it is not hard to verify that among all compact embedded surfaces of genus 0, the round sphere with radius $R = 2/c_0$ corresponds to the least minimum of the Helfrich functional (1.5) from the Alexandrov theorem [4]. In other words, all compact embedded surfaces of genus 0 have energies no less than $4\pi\bar{k}$ for positive c_0. What will happen for $c_0 < 0$ or for embedded surfaces of nonvanishing genus? This is still an open question.

We are lack of good enough mathematical tools to deal with the Helfrich functional since the Helfrich functional, different from the Willmore functional, is not an invariant under conformal transformations. However, every coin has two sides. The breaking of conformal invariance also brings benefit to us. The critical configuration

corresponding to the minimal value of the Helfrich functional should have the specific size. Introduce a scaling transformation $\mathbf{r} \to \Lambda\mathbf{r}$, where $\mathbf{r}$ represents the position vector of point on the critical configuration. Under the scaling transformation, the Helfrich functional is transformed into

$$F_H(\Lambda) = \int_M [(k_c/2)(2H)^2 + \bar{k}K]\mathrm{d}A + 2k_c c_0 \Lambda \int_M H\mathrm{d}A + (k_c c_0^2/2)\Lambda^2 \int_M \mathrm{d}A. \tag{7.1}$$

The critical configuration corresponds to $\Lambda = 1$, which implies that $F_H(\Lambda)$ takes minimal value when $\Lambda = 1$. If $c_0 \neq 0$, we may derive the necessary condition of the critical configuration:

$$\bar{H} \equiv \frac{\int_M H\mathrm{d}A}{\int_M \mathrm{d}A} = -\frac{c_0}{2}. \tag{7.2}$$

This necessary condition is quite similar to the known Minkowski formula [65]. In addition, the critical configuration of the Helfrich functional should also satisfy the shape Eq. (3.3) with vanishing p and λ. Integrating this equation and considering the Stokes theorem, we can obtain

$$\int_M H(4H^2 - 4K - c_0^2)\mathrm{d}A = 4\pi c_0 \chi(M), \tag{7.3}$$

where $\chi(M)$ is the characteristic number of surface M. The above Eqs. (7.2) and (7.3) might be helpful to the further study of the Helfrich functional.

Acknowledgments The authors are grateful to the financial support from the National Natural Science Foundation of China (Grant Nos. 11274046 and 10704009).

References

1. Plateau, J.: Statique Expérimentale et Théorique des Liquides Soumis aux Seules Forces Moléculaires. Gauthier-Villars, Paris (1873)
2. Young, T.: An essay on the cohesion of fluids. Philos. Trans. R. Soc. Lond. **95**, 65–87 (1805)
3. Laplace, P.: Traité de Mécanique Céleste. Gauthier-Villars, Paris (1839)
4. Alexandrov, A.: Uniqueness theorems for surfaces in the large. Amer. Math. Soc. transl. **21**, 341–416 (1962)
5. Poisson, S.: Traité de Mécanique. Bachelier, Paris (1833)
6. Willmore, T.: Total Curvature in Riemannian Geometry. Wiley, New York (1982)
7. Marques, F., Neves, A.: The Willmore conjecture. Jahresber. Dtsch. Math-Ver. **116**, 201–222 (2014)
8. Willmore, T.: Note on embedded surfaces. An. Ştiinţ. Univ. 'Al.I. Cuza' Iaşi, Mat. (N.S.) B **11**, 493–496 (1965)
9. Marques, F., Neves, A.: Min-max theory and the Willmore conjecture. Ann. Math. **179**, 683–782 (2014)

10. Canham, P.: The minimum energy of bending as a possible explanation of the biconcave shape of the human red blood cell. J. Theor. Biol. **26**, 61–81 (1970)
11. Singer, S., Nicolson, G.: The fluid mosaic model of cell membranes. Science **175**, 720–731 (1972)
12. Helfrich, W.: Elastic properties of lipid bilayers-theory and possible experiments. Z. Naturforsch. C **28**, 693–703 (1973)
13. Deuling, H., Helfrich, W.: Red blood cell shapes as explained on the basis of curvature elasticity. Biophys. J. **16**, 861–868 (1976)
14. Lipowsky, R.: The conformation of membranes. Nature **349**, 475–481 (1991)
15. Ou-Yang, Z., Liu, J., Xie, Y.: Geometric Methods in the Elastic Theory of Membranes in Liquid Crystal Phases. World Scientific, Singapore (1999)
16. Seifert, U.: Configurations of fluid membranes and vesicles. Adv. Phys. **46**, 13–137 (1997)
17. Chern, S., Chen, W.: Lecture on Differential Geometry. Beijing University Press, Beijing (1983)
18. Tu, Z., Ou-Yang, Z.: Lipid membranes with free edges. Phys. Rev. E **68**, 061915 (2003)
19. Tu, Z., Ou-Yang, Z.: A geometric theory on the elasticity of bio-membranes. J. Phys. A Math. Gen. **37**, 11407–11429 (2004)
20. Tu, Z., Ou-Yang, Z.: Elastic theory of low-dimensional continua and its applications in bio- and nano-structures. J. Comput. Theor. Nanosci. **5**, 422–448 (2008)
21. Westenholz, C.: Differential Forms in Mathematical Physics. North-Holland, Amsterdam (1981)
22. Ou-Yang, Z., Helfrich, W.: Instability and deformation of a spherical vesicle by pressure. Phys. Rev. Lett. **59**, 2486–2488 (1987)
23. Ou-Yang, Z., Helfrich, W.: Bending energy of vesicle membranes: general expressions for the first, second, and third variation of the shape energy and applications to spheres and cylinders. Phys. Rev. A **39**, 5280–5288 (1989)
24. Hu, J., Ou-Yang, Z.: Shape equations of the axisymmetric vesicles. Phys. Rev. E **47**, 461–467 (1993)
25. Zheng, W., Liu, J.: Helfrich shape equation for axisymmetric vesicles as a first integral. Phys. Rev. E **48**, 2856–2860 (1993)
26. Naito, H., Okuda, M., Ou-Yang, Z.: New solutions to the helfrich variation problem for the shapes of lipid bilayer vesicles: beyond delaunay's surfaces. Phys. Rev. Lett. **74**, 4345–4348 (1995)
27. Mladenov, I.: New solutions of the shape equation. Eur. Phys. J. B **29**, 327–330 (2002)
28. Ou-Yang, Z.: Anchor ring-vesicle membranes. Phys. Rev. A **41**, 4517–4520 (1990)
29. Ou-Yang, Z.: Selection of toroidal shape of partially polymerized membranes. Phys. Rev. E **47**, 747–749 (1993)
30. Castro-Villarreal, P., Guven, J.: Inverted catenoid as a fluid membrane with two points pulled together. Phys. Rev. E **76**, 011922 (2007)
31. Zhang, S., Ou-Yang, Z.: Periodic cylindrical surface solution for fluid bilayer membranes. Phys. Rev. E **53**, 4206–4208 (1996)
32. Vassilev, V., Djondjorov, P., Mladenov, I.: Cylindrical equilibrium shapes of fluid membranes. J. Phys. A Math. Theor. **41**, 435201 (2008)
33. Zhou, X.: Periodic-cylinder vesicle with minimal energy. Chin. Phys. B **19**, 058702 (2010)
34. Naito, H., Okuda, M., Ou-Yang, Z.: Counterexample to some shape equations for axisymmetric vesicles. Phys. Rev. E **48**, 2304–2307 (1993)
35. Naito, H., Okuda, M., Ou-Yang, Z.: Polygonal shape transformation of a circular biconcave vesicle induced by osmotic pressure. Phys. Rev. E **54**, 2816–2826 (1996)
36. Mutz, M., Bensimon, D.: Observation of toroidal vesicles. Phys. Rev. A **43**, 4525–4527 (1991)
37. Seifert, U.: Vesicles of toroidal topology. Phys. Rev. Lett. **66**, 2404–2407 (1991)
38. Fourcade, B., Mutz, M., Bensimon, D.: Experimental and theoretical study of toroidal vesicles. Phys. Rev. Lett. **68**, 2551–2554 (1992)
39. Evans, E., Fung, Y.: Improved measurements of the erythrocyte geometry. Microvasc. Res. **4**, 335–347 (1972)

40. Saitoh, A., Takiguchi, K., Tanaka, Y., Hotani, H.: Opening-up of liposomal membranes by Talin. Proc. Natl. Acad. Sci. **95**, 1026–1031 (1998)
41. Capovilla, R., Guven, J., Santiago, J.: Lipid membranes with an edge. Phys. Rev. E **66**, 021607 (2002)
42. Tu, Z.: Compatibility between shape equation and boundary conditions of lipid membranes with free edges. J. Chem. Phys. **132**, 084111 (2010)
43. Umeda, T., Suezaki, Y., Takiguchi, K., Hotani, H.: Theoretical analysis of opening-up vesicles with single and two holes. Phys. Rev. E **71**, 011913 (2005)
44. Wang, X., Du, Q.: Modelling and simulations of multi-component lipid membranes and open membranes via diffuse interface approaches. J. Math. Biol. **56**, 347–371 (2008)
45. Tu, Z.: Geometry of membranes. J. Geom. Symmetry Phys. **24**, 45–75 (2011)
46. Tu, Z.: Challenges in theoretical investigations of configurations of lipid membranes. Chin. Phys. B **22**, 028701 (2013)
47. Tu, Z., Ou-Yang, Z.: Recent theoretical advances in elasticity of membranes following Helfrich's spontaneous curvature model. Adv. Colloid Interface Sci. **208**, 66–75 (2014)
48. Koch, E., Fischer, W.: Flat points of minimal balance surfaces. Acta Cryst. A **46**, 33–40 (1990)
49. Giomi, L., Mahadevan, L.: Minimal surfaces bounded by elastic lines. Proc. R. Soc. A **468**, 1851–1864 (2012)
50. Capovilla, R., Guven, J.: Stresses in lipid membranes. J. Phys. A: Math. Gen. **35**, 6233–6247 (2002)
51. Müller, M., Deserno, M., Guven, J.: Interface-mediated interactions between particles: a geometrical approach. Phys. Rev. E **72**, 061407 (2005)
52. Müller, M., Deserno, M., Guven, J.: Balancing torques in membrane-mediated interactions: exact results and numerical illustrations. Phys. Rev. E **76**, 011921 (2007)
53. Deserno, M.: Fluid lipid membranes: from differential geometry to curvature stresses. Chem. Phys. Lipids **185**, 11–45 (2015)
54. Yang, P., Tu, Z.: General neck condition for the limit shape of budding vesicles. arXiv:1508.02151
55. Jülicher, F., Lipowsky, R.: Shape transformations of vesicles with intramembrane domains. Phys. Rev. E **53**, 2670–2683 (1996)
56. Du, Q., Guven, J., Tu, Z., Vázquez-Montejo, P.: Fluid membranes bounded by semi-flexible polymers (in preparation)
57. Naito, H., Okuda, M., Ou-Yang, Z.: Equilibrium shapes of smectic-A phase grown from isotropic phase. Phys. Rev. Lett. **70**, 2912–2915 (1993)
58. Naito, H., Okuda, M., Ou-Yang, Z.: Preferred equilibrium structures of a smectic-A phase grown from an isotropic phase: origin of focal conic domains. Phys. Rev. E **52**, 2095–2098 (1995)
59. Ou-Yang, Z., Su, Z., Wang, C.: Coil formation in multishell carbon nanotubes: competition between curvature elasticity and interlayer adhesion. Phys. Rev. Lett. **78**, 4055–4058 (1997)
60. Yan, X., Cui, Y., He, Q., Wang, K., Li, J., Mu, W., Wang, B., Ou-Yang, Z.: Reversible transitions between peptide nanotubes and vesicle-like structures including theoretical modeling studies. Chem. Eur. J. **14**, 5974–5980 (2008)
61. Friedel, G.: Les états mésomorphes de la matiére. Ann. Phys. **18**, 273–474 (1922)
62. Bragg, W.: Liquid crystals. Nature **133**, 445–456 (1934)
63. Langer, J., Singer, D.: The total squared curvature of closed curves. J. Differ. Geom. **20**, 1–22 (1984)
64. Zhang, X., Zhang, X., Bernaerts, D., Vantendeloo, G., Amelinckx, S., Vanlanduyt, J., Ivanov, V., Nagy, J., Lambin, P., Lucas, A.: The texture of catalytically grown coil-shaped carbon nanotubules. Europhys. Lett. **27**, 141–146 (1994)
65. Sabitov, I.: Some integral formulas for compact surfaces. TWMS J. Pure Appl. Math. **1**, 123–131 (2010)